Engineering Science and Technology, an International Journal 19 (2016) 1457–1464

HOSTED BY

ELSEVIER

Contents lists available at ScienceDirect

Engineering Science and Technology, an International Journal

journal homepage: www.elsevier.com/locate/jestch

Full Length Article

Classification of motor imagery movements using multivariate empirical mode decomposition and short time Fourier transform based hybrid method

Syed Khairul Bashar *, Mohammed Imamul Hassan Bhuiyan

Department of Electrical and Electronic Engineering, Bangladesh University of Engineering and Technology, Bangladesh

ARTICLE INFO

Article history:
Received 28 March 2016
Revised 29 April 2016
Accepted 29 April 2016
Available online 9 May 2016

Keywords:
Electroencephalogram (EEG)
Multivariate EMD
Energy
Short time Fourier transform
kNN classifier

ABSTRACT

Effective online processing of electroencephalogram (EEG) signals is a prerequisite of brain computer interfacing (BCI). In this paper, we propose a hybrid method consisting of multivariate empirical mode decomposition (MEMD) and short time Fourier transform (STFT) to identify left and right hand imaginary movements from EEG signals. Experiments are carried out using the publicly available benchmark BCI competition II Graz motor imagery data base. The EEG epochs are decomposed into multiple intrinsic mode functions (IMFs) by applying MEMD. The most significant mode is subjected to the short time Fourier transform; the peak of the magnitude spectrum is used as feature representing the corresponding epoch. The efficacy of the proposed feature extraction scheme is demonstrated by intuitive, statistical and graphical analyses. The performance of the proposed feature extraction scheme is investigated for various choices of classifiers. Our findings suggest that k-Nearest Neighbor (kNN) emerges as the best classification model yielding 90.71% accuracy. The performance of our method is also compared to that of existing works in the literature. Experimental outcomes backed by statistical validation manifest that the performance of the proposed method is comparable or better than many of the state-of-the-art algorithms.

1. Introduction

Brain computer interfacing allows to control and operate computer aided systems by intent alone. The major objective of BCI is to assist disable people for their rehabilitation. BCI involves detection, analysis and classification of different types of motor imagery movements to implement real time control and communication. Electroencephalogram (EEG) signals are often used for BCI purpose since it can be implemented as a non-invasive system [1].

There are several categories of EEG-based BCI such as limb motor imagery classification [2], continuous arm movements direction detection [3], individual finger movement decoding [4], forward–backward hand movement prediction [5], P300 evoked potential based character recognition [6] etc. One major category of BCI is the detection of motor imagery movements such as left and right hand movements [7]. Various methods have been developed in the literature for classifying different types of arm movements. A wavelet-based common spatial pattern (CSP) algorithm using low frequency features and Fisher linear discriminant classifier is developed to classify fast and slow hand movements in [8]. In [9], filter bank common spatial pattern (FBCSP) is implemented with mutual information based feature selection and for the identification task, Naive Bayesian Parzen Window (NBPW) classifier is used. Wrist movement classification has been done by extracting gamma band features from wavelet packet transform and employing radial basis function (RBF) classifier in [10]. Separability of EEG signals using adaptive auto regressive parameters is proposed in [11]. Time–frequency optimization and linear discriminant analysis is performed to classify left and right hand movements with reduced electrodes in [12].

Since EEG data for research purpose can be acquired with varying experimental setup and conditions, BCI competition was held providing standard data sets to evaluate and compare different algorithms. The standard data sets are proved to be representative in motor imagery and are suitable for BCI research. Different approaches have been studied to classify motor imagery movements in BCI competition II Graz motor imagery data set. Band passed EEG signals and power spectral density based linear discriminant analysis (LDA) is proposed in [13]. A Hidden Markov Model (HMM) based method is presented in [14] by the same author. Adaptive Auto Regressive (AAR) model based features are

* Corresponding author.
E-mail address: s.k.bashar@ieee.org (S.K. Bashar).
Peer review under responsibility of Karabuk University.

http://dx.doi.org/10.1016/j.jestch.2016.04.009
2215-0986/

used with Bayesian Graphical Network (BGN) and Multi Layer Perceptron classifiers in [15,16]. Morlet wavelet is used to extract features from mu rhythms that are used in Bayes quadratic classifiers in [17]. Wavelet coefficient based statistical features and fuzzy support vector machine (FSVM) classifier is described in [18]. Discrete wavelet transform (DWT) along with autoregressive (AR) model is used to classify hand movements in [19]. In [20], higher order statistical features based on bi-spectrum of EEG signals are extracted to classify mental tasks. Multiple auto-correlation based feature extraction method along with learning vector quantization (LVQ) is proposed in [21]. Most recently, discriminative area selection (DAS) method is implemented with fuzzy Hopfield neural network (FHNN) classifier in [22].

To the best of authors' knowledge, a hybrid of multivariate EMD and short time Fourier transform is applied for the first time in EEG signal processing. The objective of this work is to identify imagery hand movements by extracting suitable features from EEG signals. Since EEG signal is invariably nonlinear and non-stationary [23], fixed linear orthogonal basis functions are not suitable for real life EEG data. The underlying dynamics of EEG signals is spread over various sub-bands in the frequency domain and particularly for motor imagery analysis, mu (8–12 Hz) and beta (18–25 Hz) rhythms have significant importance in neurophysiological context [24]. Empirical mode decomposition (EMD) has been successfully utilized in the processing of EEG signals [25,26]. It requires no pre-defined basis functions as in Fourier or traditional time–frequency transforms. However, EEG signals are usually multi-channel type whereas the EMD is applied on a single-channel basis; thus it ignores cross-channel dependence. Recently, the multivariate EMD (MEMD) has been introduced which can capture the cross-channel dependency and can be applied directly to all the EEG channels. Thus, in this paper the multi-channel EEG signal is decomposed into various intrinsic mode functions (IMFs) using MEMD. In addition, the 3rd IMF is shown to be most significant in terms of energy. Furthermore, in order to obtain localized information, the most significant intrinsic mode function is subjected to STFT and the peaks of the magnitude spectrum are used as features. The justification of the extracted features by this hybrid method is provided through statistical analysis (ANOVA and Kruskal–Wallis test) and graphical representations such as scatter plots, box plots and histograms. The features are then employed in the kNN classifier to discriminate left and right hand imagery movements. The performance of the proposed method is extensively studied for different classifiers and compared with that of other existing techniques.

2. Description of the EEG database

BCI competition II data set (GRAZ motor imagery III) provided by Technical University of Graz is used in this paper. The data is acquired from a normal subject while the subject is sitting in a chair with armrests. The subject is trying to control a feedback bar by making imagery movements of left or right hands. Left and right cues are in random order [27]. 7 runs are used with 40 trials for each run. During each trial at 2 s, an acoustic stimulus indicates the beginning of the trial and a cross '+' is displayed for 1 s. After this an arrow (left or right) is displayed at 3 s as the cue. At the same time the subject is asked to move a bar into the direction of the cue which is controlled by adaptive autoregressive parameters of channel C3 and C4. The EEG signal is filtered between 0.5 and 30 Hz while the sampling rate is 128 Hz. The data set has both training and testing trial sets (containing 140 trials in each set) which are randomly selected to prevent any systematic effect due to feedback. The 140 train trials are provided with labels using which the test labels are to be determined. Fig. 1(a) shows the timing scheme of the experimental

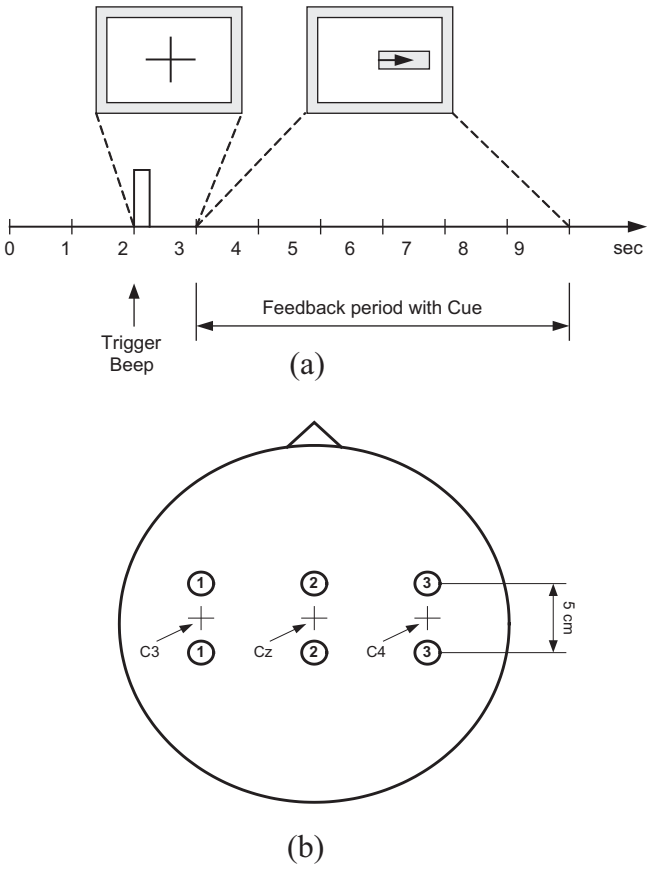

Fig. 1. (a) Timing scheme of the experiment; (b) electrode positions.

procedure while Fig. 1(b) presents the electrodes position of the EEG signal acquisition system. A detail description of the data set can be found in [28].

3. Multivariate empirical mode decomposition

Empirical mode decomposition (EMD) is a data driven technique to decompose a signal into a finite set of band limited basis functions called intrinsic mode functions (IMFs) [29]. The multivariate empirical mode decomposition (MEMD) is recently developed, where instead of computing the local mean using the average of upper and lower envelopes like conventional EMD, the multiple n dimensional envelopes are generated by projecting the signal along every directions in n variate spaces in MEMD. These projections are averaged to obtain the local mean.

Let a multivariate signal with n components is denoted by n dimensional vectors $\{\mathbf{v}(t)\}_{t=1}^{T} = \{v_1(t), v_2(t), \ldots, v_n(t)\}$ where $\mathbf{x}^{\theta_k} = x_1^k, x_2^k, \ldots, x_n^k$ denotes a set of direction vectors along the directions given by angles $\theta^k = \{\theta_1^k, \theta_2^k, \ldots, \theta_{(n-1)}^k\}$ on an $(n-1)$ sphere. The steps to compute MEMD is given below [30]:

1. Select suitable points for sampling on an $(n-1)$ sphere.
2. Calculate projection $\{p^{\theta_k(t)}\}_{t=1}^{T}$ along the direction vector $\mathbf{x}^{\theta_k}$ of the input signal $\{\mathbf{v}(t)\}_{t=1}^{T}$ for all k resulting $\{p^{\theta_k(t)}\}_{k=1}^{K}$ as the projection set.
3. Find the time instants $\{t_i^{\theta_k}\}$ corresponding to the maxima of $\{p^{\theta_k(t)}\}_{k=1}^{K}$.
4. Interpolate $[t_i^{\theta_k}, \mathbf{v}(t_i^{\theta_k})]$ to obtain multivariate envelope curves $\{\mathbf{e}^{\theta_k}(t)\}_{k=1}^{K}$.

5. Calculate the mean $\mathbf{m}(t)$ of the envelopes for K direction vectors as

$$\mathbf{m}(t) = \frac{1}{K}\sum_{k=1}^{K}\mathbf{e}^{\theta_k}(t). \quad (1)$$

6. Extract the detail $d(t)$ using $d(t) = x(t) - m(t)$. If $d(t)$ fulfills the stoppage criterion for the IMF, apply the procedure to $x(t) - d(t)$, else apply it to $d(t)$.

Fig. 2 shows the original EEG signals collected from C3, Cz and C4 channels, respectively. In Fig. 3, 8 IMFs for each channel generated from MEMD are presented where Fig. 3(a)–(c) show the IMFs corresponding to C3, C4 and Cz channels, respectively.

4. Analysis in multivariate EMD domain

The multivariate EMD of the EEG signal leads to multiple intrinsic mode functions (IMFs). In this study eight IMFs have been extracted from EEG signal. However, since all IMFs do not change equally during the two specific movements, they do not have equal energy. As a result, not all the IMFs are equally significant in the detection of left and right hand imagery movements. To select the most significant IMF, we have analyzed the energy variation of the corresponding IMFs in the same channel during left and right hand movements. Fig. 4(a) shows that the energy of the third IMF is significantly greater than any other IMF for left and right hand movements. Fig. 4(b) shows the energy variation in 8 IMFs during two imagery movements for all the train data base. It is seen that energy of the third IMF changes significantly during the two specific motor imagery movements while for the other seven IMFs, the change is not appreciable. Since the third IMF has maximum energy and most significant energy variation, it is selected for further analysis.

The selection of the third IMF has two advantages. First, it enables to reduce the feature dimension by selecting only one IMF out of eight. Second, by selecting the IMF corresponding to largest energy variation for the two specific movements as well as maximum energy, the features extracted from this IMF are expected to have better discriminating ability.

4.1. Feature extraction from the IMFs

Fig. 5(a) shows the third IMF of MEMD for the two specific movements. The activation of brain signals for left and right hand differs in time frequency scale in the IMF and from Fig. 5(a), it is clear that two signals do not have same range of oscillations at the same time indicating the signals are effective in different times. To separate them by extracting suitable features, we need to look for the "activated" frequency components of these signals. For analyzing the activated frequency components, power spectral density (PSD) is obtained for these two signals. One can see from Fig. 5(b) that PSD of left and right hand imagery movements are quite similar. It indicates that these signals do not have distinguishing features in the Fourier domain. To extract effective features for separating these, we need to perform time frequency analysis to know in which time what frequency components are more activate. For analyzing the time frequency property, well established short time Fourier transform (STFT) is used which gives the opportunity to view signal spectrum at different time frames or windows.

Short time Fourier transform is a process to observe how the frequency content of a signal changes over time [31]. It is calculated by dividing the long signal into shorter time segments and then computing the spectrum of each segments or frames. If the signal $x(t)$ is pre-windowed around a time instant t and the Fourier

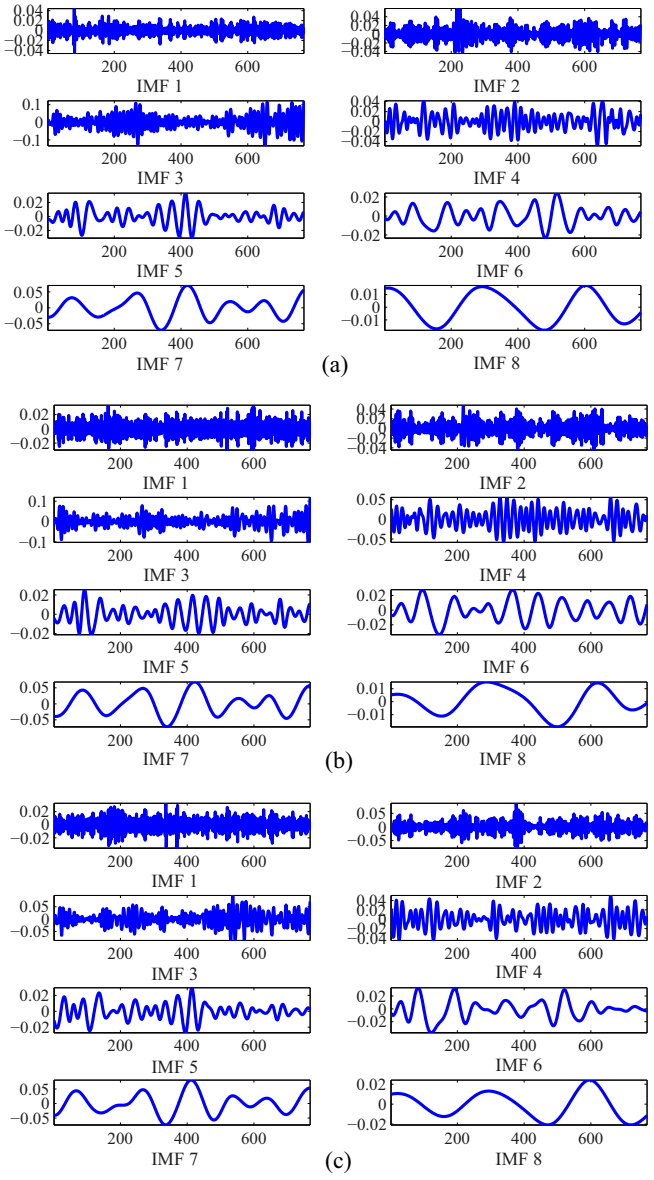

Fig. 3. 8 IMFs of EEG signal from (a) C3 channel, (b) Cz channel and (c) C4 channel, respectively.

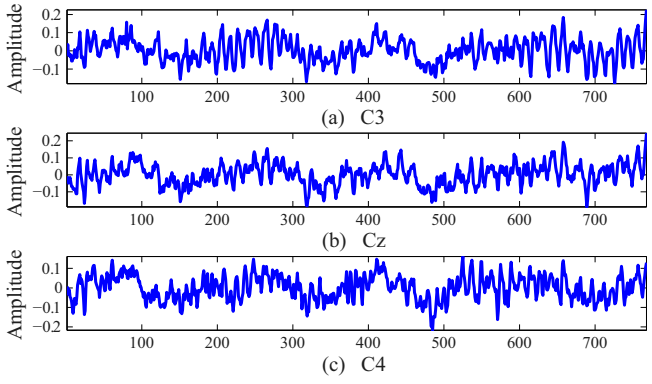

Fig. 2. Original EEG signals: collected from (a) C3 channel, (b) Cz channel and (c) C4 channel, respectively.

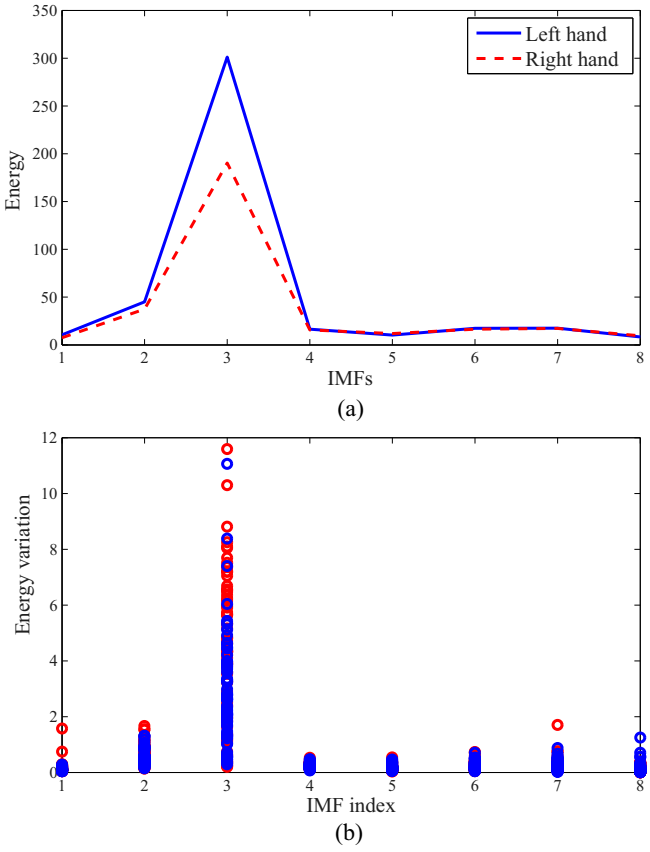

Fig. 4. (a) Energy of all the 8 IMFs, (b) energy variation in 8 IMFs during two movements on train data.

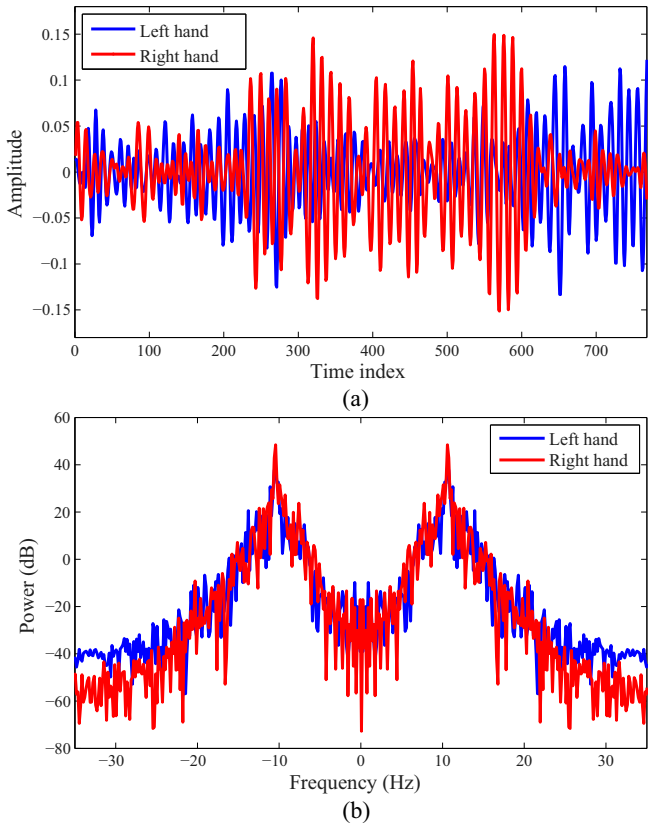

Fig. 5. (a) Third IMF for left and right hand imagery movements, (b) PSD of third IMF for left and right hand movements.

transform is calculated at each time instant t, then the STFT of the signal $x(t)$ is expressed as,

$$STFT(t,f) = \int_{-\infty}^{+\infty} x(\tau)h(\tau - t)e^{-if\tau}d\tau \tag{2}$$

where $h(t)$ is the window function [32].

In this work, the STFT is applied to the 3rd IMF for 8 frames where the Fourier transform is calculated in each frame of the IMF. Let "$S_N(c)$" denotes the STFT outputs where N indicates the frame number and c is the channel index (i.e., $C3$ or $C4$). For example, $S_1(C4)$ indicates first frame of the STFT for $C4$ channel. Fig. 6 (a)–(c) represent the magnitude spectrum of $S_2(C3), S_3(C3)$ and $S_4(C3)$ of the third IMF, respectively. From those figures it is easily visible that the magnitude spectrum of $S_2(C3), S_3(C3)$ and $S_4(C3)$ of the third IMF is clearly distinguishable for left and right hand imagery movements and in particular, the peak values for left hand movements are much higher than for right hand imagery movements in these three frames (i.e., second, third and fourth frames). As a result, the sum of these three peaks has been used as the feature. Instead of using three peaks separately as features, the sum provides extra advantages. It gives emphasis to all three peak values and not particularly one. Moreover, using the sum as feature, the feature dimension for a single channel is reduced to one from three compared to separately using the three peaks.

If FT indicates the feature vector, then it can be expressed as

$$FT = [F(C3), F(C4)]^T \tag{3}$$

where $F(C3)$ and $F(C4)$ are the sum of the peak values of the magnitude spectra for $C3$ and $C4$ channels from second to fourth frame, respectively and can be expressed as

$$\begin{aligned} F(C3) &= \sum_{N=2}^{4} max\,(abs\,(S_N(C3))) \\ F(C4) &= \sum_{N=2}^{4} max\,(abs\,(S_N(C4))) \end{aligned} \tag{4}$$

here, *max* indicates the maximum value while *abs* signifies the absolute value of $S_N(c)$, also known as the magnitude spectrum of the STFT.

The feature quality of FT has been statistically justified using one way analysis of variance (ANOVA) and Kruskal–Wallis [33] p-values. The p-values of ANOVA and Kruskal–Wallis hypothesis testing for left and right hand imagery movements on train data set have been given in Table 1. The hypothesis about the p-values is that the value, $p < 0.05$ indicates that at least one sample mean is significantly different than the other sample means statistically [34]. From Table 1, it is clear that the p-values are very small. Hence it can be concluded that the features have good distinguishable property statistically.

In Table 2, we have given p-values of the features for both ANOVA and Kruskal–Wallis methods if one step analysis is performed. Single step features include maximum of IMF3 (for only MEMD method) and maximum of absolute value of STFT 4th frame (for only STFT method which is directly performed on original EEG epochs without MEMD). The two steps hybrid features show smaller p-values than the single step features which justifies the proposed ones as superior features.

Apart from ANOVA and Kruskal–Wallis p-values, scatter plots, box plots and histograms are provided to further illustrate the classification property of the extracted features. Fig. 7 represents the scatter plots of $F(C3)$ and $F(C4)$ features. In Fig. 7, blue circles and green squares indicate feature values during left and right

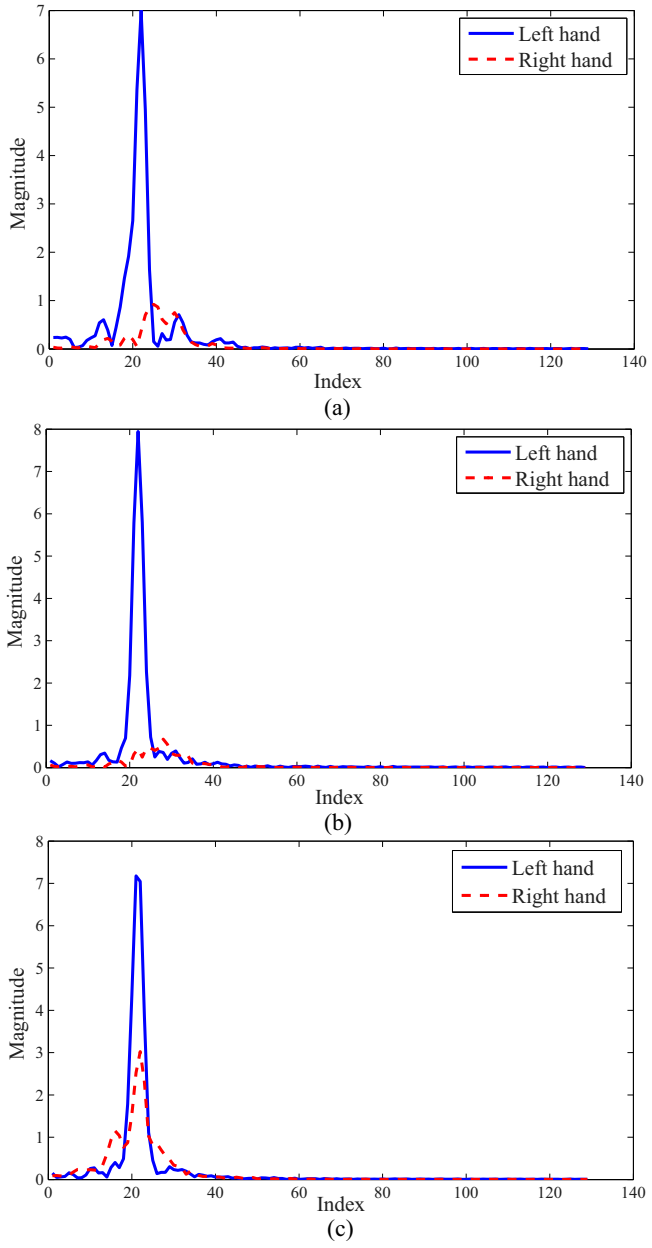

Fig. 6. Magnitude spectrum of the STFT of (a) 2nd, (b) 3rd and (c) 4th frame, respectively.

Table 1
p-Values of the features.

Analysis name	Features	*p*-Values
One way ANOVA	F(C3)	8.2750e−08
	F(C4)	1.2687e−08
Kruskal–Wallis method	F(C3)	6.5038e−06
	F(C4)	6.6207e−08

hand imagery movements, respectively. Here, the green and blue markers have significantly different values which indicate the variation during different imagery hand movements and as a result, they can be regarded as good separable features to be used in classifiers.

Fig. 8(a) and (b) show the box plots of $F(C3)$ and $F(C4)$, respectively for left and right hand imagery movements on the train data set. The box plots have non overlapping notches which indicates that the features have distinct values for the two specific movements.

Table 2
Comparison of *p*-values for different methods.

Analysis name	Features	*p*-Values for different methods		
		MEMD	STFT	Hybrid
One-way ANOVA	F(C3)	0.1253	2.5656e−04	8.2750e−08
	F(C4)	0.0680	0.6989e−05	1.2687e−08
Kruskal–Wallis method	F(C4)	0.0387	6.2259e−04	6.5038e−06
	F(C3)	0.0613	2.1142e−04	6.6207e−08

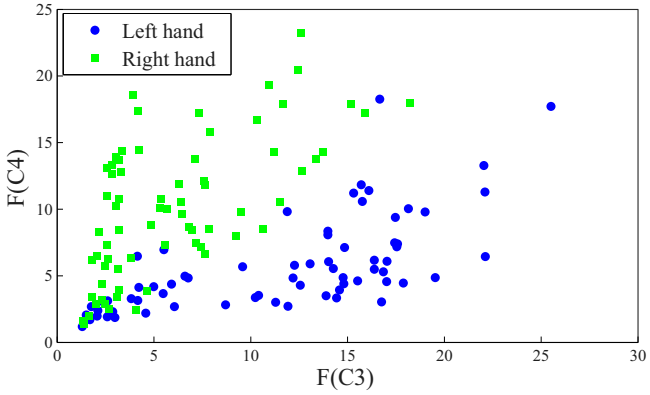

Fig. 7. Scatter plots for $F(C3)$ and $F(C4)$ for two imagery movements.

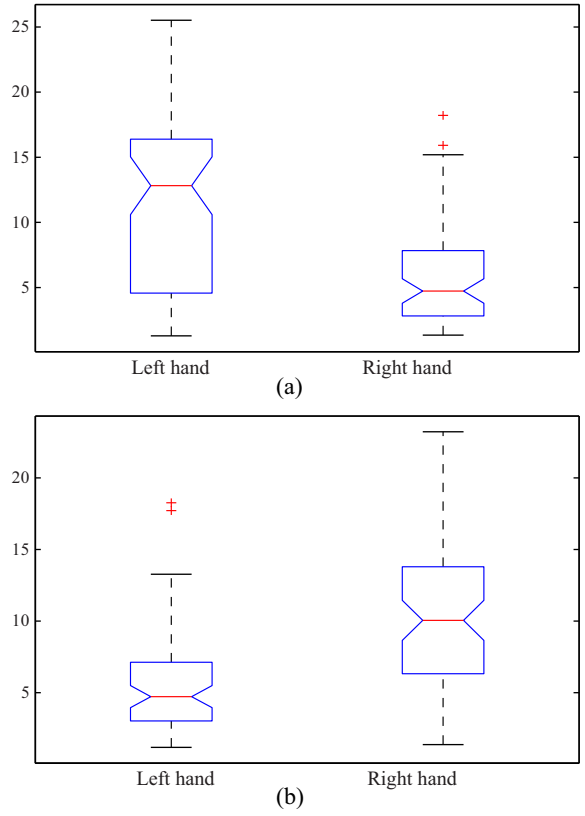

Fig. 8. Box plots of (a) $F(C3)$ and (b) $F(C4)$ for left and right hand movements, respectively.

Fig. 9 presents the histograms of $F(C3)$ and $F(C4)$ during left and right hand imagery movements on training data where red and green color indicate left and right hand, respectively. From the histograms, it can be concluded that the corresponding histograms have peaks in different regions which is the evidence that the features show different values during two specified motor imagery movements. For example, $F(C4)$ has peak around 5 for left hand imagery movements while for right hand imagery movements, it has sort of uniform distribution in 0–20 region.

The scatter plots, box plots, histograms and the p-values of one way ANOVA as well as Kruskal–Wallis analysis justify both graphically and statistically that the extracted features (i.e., $F(C3)$ and $F(C4)$) have significantly distinguishable values for left and right hand motor imagery movements. In other words, the features have good between-class distance and small within-class variance in the feature vector space [35] and as a result, they can be used as suitable features to classify two hand movements.

4.2. Classification using the kNN classifier

For any classification problem, there are two main parts – feature extraction and classification. Feature extraction is the method of calculating any measure which can represent the observed signal [36]. If suitable features can be extracted, then a simple classifier can provide the desired outcome. Among different classifiers, kNN classifier performs best in our study. k-Nearest Neighbors algorithm (kNN) is a non-parametric learning algorithm method used for classification. Among the various methods of supervised statistical pattern recognition, the Nearest Neighbor rule achieves consistently high performance, without a priori assumptions about the distributions from which the training examples are drawn [37]. In order to classify a sample trial vector X which has unknown class, kNN classifier ranks the sample trial's neighbors among the training trial vectors and uses the class labels of the K most similar neighbors to predict the class of the new test trial [38]. The classes of these neighbors are then weighted according to the similarity of each neighbor where the similarity index is the cosine value between two sample vectors of Euclidean distance. The cosine similarity index is defined as

$$sim(X, D_j) = \frac{\sum_{t_i \in (X \cap D_j)} x_i \times d_{ij}}{||X||_2 \times ||D_j||_2} \quad (5)$$

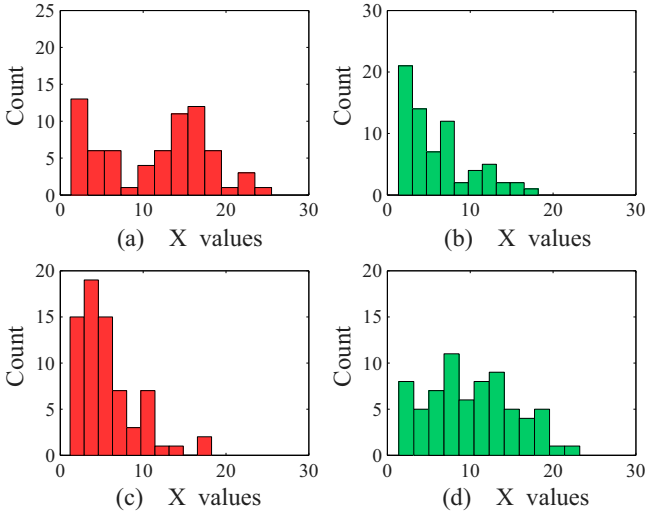

Fig. 9. (a), (b) Histograms of $F(C3)$ for left and right hand imagery movements, respectively; (c), (d) histograms of $F(C4)$ for left and right hand imagery movements, respectively.

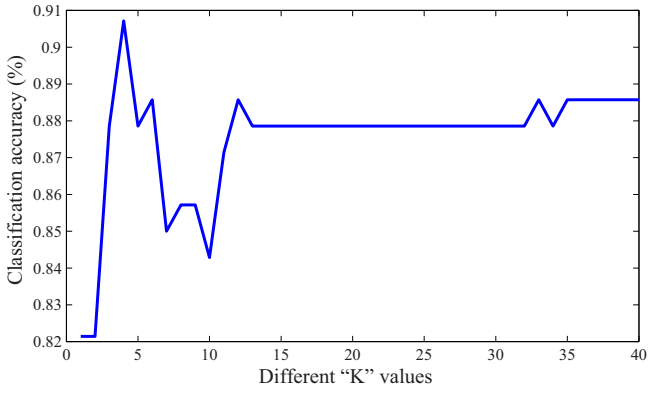

Fig. 10. Classification accuracy (%) vs different "K" values.

where X is the test or unknown trial; D_j is the jth training trial; t_i is shared by both X and D_j; d_{ij} is the weight for t_i in training sample D_j whereas x_i is the weight for t_i in X. The l_2 norm of X is defined as

$$||X||_2 = \sqrt{x_1^2 + x_2^2 + x_3^2 + \cdots} \quad (6)$$

The number "K" decides how many neighbors influence the classification. If $k = 1$, then the algorithm is simply called the nearest neighbor algorithm.

5. Experimental analysis

The BCI competition II Graz motor imagery EEG data set has 140 trials each for left and right hand (total 280 trials) of 9 s length.

Table 3
Confusion matrix of left and right hand movements classification.

	Predicted labels			
Ground truth		Left	Right	Sensitivity
	Left	60	10	85.71%
	Right	3	67	95.71%

Table 4
Performance Evaluation of different classifiers.

Classifier name	Parameter	Classification accuracy (%)
Discriminant analysis	Linear distance	85.71
	Diaglinear distance	85.00
	Quadratic distance	85.71
	Diagquadratic distance	85.00
	Mahalanobis distance	85.71
Naive Bayes	Normal distribution	85.00
SVM	Linear kernel	86.43
	Radial basis	87.14
PNN	Radial basis network	87.14
GRNN	Radial basis network	87.14
ANFIS	Subtractive clustering ("hybrid")	85.71
	Subtractive clustering (back propagation)	86.43
	C-means clustering ("hybrid")	86.43
	C-means clustering (back propagation)	86.43
kNN	Euclidean distance	85.71
	Cityblock distance	85.71
	Correlation distance	89.29
	Cosine distance	90.71

Table 5
Comparison of classification accuracy of different methods.

Method	Proposed by	Classifier	Classification accuracy (%)
PSD	Solhjoo et al. [13]	Mahalanobis distance	63.1
		Gaussian classifiers	65.4
		LDA	65.6
AAR	Tavakolian et al. [16]	Bayes quadratic	82.86
		BGN	83.57
		MLP	84.29
Morlet wavelet	Lemm et al. [17]	Bayes quadratic	89.29
Wavelet based features	Xu et al. [18]	FSVM	87.86
DWT and AR model	Xu et al. [19]	LDA	90.00
Higher order features	Zhou et al. [20]	LDA	89.29
		Neural network	90.00
Multiple auto correlation	Wang et al. [21]	LVQ	90.00
Discriminative area selection	Hsu [22]	FHNN	83.10
Proposed method (MEMD + STFT)		kNN	90.71

Since the cue was given at $t = 3$ s, data segment after 3 s from C3 and C4 channels are used for classification. So each data segment for a single channel has a duration of 6 s with $6 \times 128 = 768$ data points since the sampling frequency is 128 Hz. We have used one feature from each channel. So the number of feature element is two per epoch. Thus both the train and test feature matrices have dimension of 140×2 which is fed to kNN classifier. kNN classifier has been trained with the train data set and after training, the label of the test data set has been determined. These predicted test labels are compared with ground truth provided by BCI II organizer. It is to be noted here that all the analysis have been performed only on the train data set to determine the feature quality and for the training stage of the classifier, only the train data set has been used. The experiments are carried out using MATLAB 2013b [34] on Windows-7 32 bit platform having 1 GB RAM and 2.93 GHz Intel Core 2 Duo processor. Since the feature dimension is only two, the classification complexity is very low and using the abovementioned computer setup, it requires only 2 ms for each test trial classification. kNN classifier has two parameters to tune: the distance parameter and the "K" value. The distance parameter is selected as "cosine" which means one minus the cosine of the included angle between points [34]. Another parameter of kNN classifier is the value of "K". For choosing the optimum "K" value, we have varied the value of "K" and it is noted that for our classification problem, $K = 4$ gives the highest accuracy of 90.71%. Fig. 10 shows the variation of "Classification accuracy (%)" for different "K" values. From the figure it is clear that for $K = 4$, the classifier provides highest accuracy. The classification accuracy has been calculated as follows:

$$\textit{Classification accuracy} = \frac{\textit{Correctly classified test trials}}{\textit{Total test trials}} \times 100\% \tag{7}$$

In some literature, misclassification rate or error rate is calculated which can be measured by error rate = 100%-classification accuracy (%).

Table 3 shows the confusion matrix of the two way classification problem of left and right hand imagery movements detection where "predicted labels" are the output of the kNN classifier while "ground truth" are the test label provided by the BCI II organizer. From the confusion matrix, it can be seen that right hand classification accuracy is better than left hand. Among 70 trials for right hand, 67 are classified correctly while for left hand the correctly detected movements are 60 out of 70.

In this paper, we have also conducted performance comparison of existing classifiers employing the extracted features in the Graz motor imagery data set. The classifiers considered includes probabilistic neural network (PNN), support vector machine (SVM), generalized regression neural network (GRNN), adaptive neuro fuzzy inference system (ANFIS), discriminant analysis (DA), Naive Bayes [39] and k-Nearest Neighbor (kNN) with various parameters. Table 4 provides the outcomes of different classifiers. It is seen that kNN classifier with "cosine" distance gives better classification accuracy than other classifiers with varying parameters (for ANFIS, "hybrid" indicates the combination of least squares with back propagation).

Finally, Table 5 compares the classification accuracy of the proposed method with those of the several other existing methods. It is observed that using simple kNN classifier, the proposed method provides better classification accuracy in detecting left and right hand motor imagery movements than others methods. Another very positive outcome of our method is that, *the feature vector dimension is only two which reduces the complexity of the classification scheme*.

6. Conclusions

In this work, the problem of distinguishing left and right hand imagery movements from EEG signals has been solved by obtaining localized information in the multivariate empirical mode decomposition and short time Fourier transform based hybrid domain. The superiority of the algorithm has been confirmed by statistical hypothesis testing and graphical analysis. The extracted features have been implemented using various learning algorithms to study the general performances of the classifiers in EEG based brain computer interfacing. The accuracy of the classification scheme is promising and the proposed algorithm has been evaluated against previously published works yielding satisfactory outcome. The computational complexity of the classification task is also practical due to low dimensional feature space. We thus come into a conclusion, as the experimental results and analysis suggest, the devised scheme is simple, yet effective and efficient.

References

[1] L.F. Nicolas-Alonso, J. Gomez-Gil, Brain computer interfaces, a review, Sensors 12 (2) (2012) 1211–1279.
[2] W. Yi, S. Qiu, H. Qi, L. Zhang, B. Wan, D. Ming, Eeg feature comparison and classification of simple and compound limb motor imagery, J. Neuroeng. Rehabil. 10 (2013).
[3] J.-S. Woo, K.-R. Muller, S.-W. Lee, Classifying directions in continuous arm movement from eeg signals, in: 3rd International Winter Conference on Brain–Computer Interface (BCI), IEEE, 2015, pp. 1–2.
[4] K. Liao, R. Xiao, J. Gonzalez, L. Ding, Decoding individual finger movements from one hand using human eeg signals.

[5] S.K. Bashar, M.I.H. Bhuiyan, Identification of arm movements using statistical features from eeg signals in wavelet packet domain, in: 2015 International Conference onElectrical Engineering and Information Communication Technology (ICEEICT), IEEE, 2015, pp. 1–5.
[6] Z. Amini, V. Abootalebi, M.T. Sadeghi, Comparison of performance of different feature extraction methods in detection of p300, Biocybern. Biomed. Eng. 33 (1) (2013) 3–20.
[7] S.K. Bashar, A.R. Hassan, M.I.H. Bhuiyan, Identification of motor imagery movements from eeg signals using dual tree complex wavelet transform, in: 2015 International Conference on Advances in Computing, Communications and Informatics (ICACCI), IEEE, 2015, pp. 290–296.
[8] N. Robinson, A.P. Vinod, K.K. Ang, K.P. Tee, C.T. Guan, Eeg-based classification of fast and slow hand movements using wavelet-csp algorithm, IEEE Trans. Biomed. Eng. 60 (8) (2013) 2123–2132.
[9] K.K. Ang, Z.Y. Chin, C. Wang, C. Guan, H. Zhang, Filter bank common spatial pattern algorithm on bci competition iv datasets 2a and 2b, Front. Neurosci. 6 (2012).
[10] Y.U. Khan, F. Sepulveda, Brain–computer interface for single-trial eeg classification for wrist movement imagery using spatial filtering in the gamma band, IET Signal Process. 4 (5) (2010) 510–517.
[11] C. Neuper, A. Schlögl, G. Pfurtscheller, Enhancement of left-right sensorimotor eeg differences during feedback-regulated motor imagery, J. Clin. Neurophysiol. 16 (4) (1999) 373–382.
[12] Y. Yang, S. Chevallier, J. Wiart, I. Bloch, Time–frequency optimization for discrimination between imagination of right and left hand movements based on two bipolar electroencephalography channels, EURASIP J. Adv. Signal Process. 2014 (1) (2014) 1–18.
[13] S. Solhjoo, M. Moradi, Mental task recognition: a comparison between some of classification methods, in: BIOSIGNAL 2004 International EURASIP Conference, 2004, pp. 24–26.
[14] S. Solhjoo, A.M. Nasrabadi, M.R.H. Golpayegani, Classification of chaotic signals using hmm classifiers: eeg-based mental task classification, in: 2005 13th European Signal Processing Conference, IEEE, 2005, pp. 1–4.
[15] K. Tavakolian, F. Vasefi, K. Naziripour, S. Rezaei, Mental task classification for brain computer interface applications, in: Canadian Student Conference on Biomedical Computing, 2006.
[16] F. Lotte, M. Congedo, A. Lécuyer, F. Lamarche, A review of classification algorithms for eeg-based brain–computer interfaces, J. Neural Eng. 4 (2007).
[17] S. Lemm, C. Schäfer, G. Curio, Bci competition 2003-data set iii: probabilistic modeling of sensorimotor μ rhythms for classification of imaginary hand movements, IEEE Trans. Biomed. Eng. 51 (6) (2004) 1077–1080.
[18] Q. Xu, H. Zhou, Y. Wang, J. Huang, Fuzzy support vector machine for classification of eeg signals using wavelet-based features, Med. Eng. Phys. 31 (7) (2009) 858–865.
[19] B. Xu, A. Song, Pattern recognition of motor imagery eeg using wavelet transform, J. Biomed. Sci. Eng. 1 (01) (2008) 64.
[20] S.-M. Zhou, J.Q. Gan, F. Sepulveda, Classifying mental tasks based on features of higher-order statistics from eeg signals in brain–computer interface, Inf. Sci. 178 (6) (2008) 1629–1640.
[21] X. Wang, A. Wang, S. Zheng, Y. Lin, M. Yu, A multiple autocorrelation analysis method for motor imagery eeg feature extraction, in: The 26th Chinese Control and Decision Conference (2014 CCDC), IEEE, 2014, pp. 3000–3004.
[22] W.-Y. Hsu, Brain–computer interface: the next frontier of telemedicine in human–computer interaction, Telematics Inf. 32 (1) (2015) 180–192.
[23] C. Park, D. Looney, A. Ahrabian, D.P. Mandic, et al., Classification of motor imagery bci using multivariate empirical mode decomposition, IEEE Trans. Neural Syst. Rehabil. Eng. 21 (1) (2013) 10–22.
[24] D.J. McFarland, L.A. Miner, T.M. Vaughan, J.R. Wolpaw, Mu and beta rhythm topographies during motor imagery and actual movements, Brain Topography 12 (3) (2000) 177–186.
[25] P.F. Diez, V. Mut, E. Laciar, A. Torres, E. Avila, Application of the empirical mode decomposition to the extraction of features from eeg signals for mental task classification, in: Engineering in Medicine and Biology Society, EMBC 2009. Annual International Conference of the IEEE, IEEE, 2009, pp. 2579–2582.
[26] S. Alam, M.I.H. Bhuiyan, Detection of seizure and epilepsy using higher order statistics in the emd domain, IEEE J. Biomed. Health Inf. 17 (2) (2013) 312–318.
[27] G. Pfurtscheller, C. Neuper, A. Schlögl, K. Lugger, Separability of eeg signals recorded during right and left motor imagery using adaptive autoregressive parameters, IEEE Trans. Rehabil. Eng. 6 (3) (1998) 316–325.
[28] Graz description of data set iii of bci-competition, 2003. <http://ww.bbci.de/competition/ii/> (2015, online).
[29] M.K.I. Molla, T. Tanaka, T.M. Rutkowski, Multivariate emd based approach to eog artifacts separation from eeg, in: 2012 IEEE International Conference on Acoustics, Speech and Signal Processing (ICASSP), IEEE, 2012, pp. 653–656.
[30] N. Rehman, D.P. Mandic, Multivariate empirical mode decomposition, in: Proceedings of The Royal Society of London A: Mathematical, Physical and Engineering Sciences, The Royal Society, 2009. rspa20090502.
[31] I. Selesnick, Short time fourier transform, Connexions, Aug 9.
[32] A.T. Tzallas, M.G. Tsipouras, D. Fotiadis, et al., Epileptic seizure detection in eegs using time–frequency analysis, IEEE Trans. Inf. Technol. Biomed. 13 (5) (2009) 703–710.
[33] W.H. Kruskal, W.A. Wallis, Use of ranks in one-criterion variance analysis, J. Am. Stat. Assoc. 47 (260) (1952) 583–621.
[34] Matlab, 2015. <http://www.mathworks.com/products/matlab/> (online).
[35] S. Theodoridis, K. Koutroumbas, Pattern Recognition (Fourth Edition), fourth edition Edition., Academic Press Elsevier, Boston, 2009.
[36] R. Jegadeeshwaran, V. Sugumaran, Brake fault diagnosis using clonal selection classification algorithm (csca)–a statistical learning approach, Engineering Science and Technology, an International Journal 18 (1) (2015) 14–23.
[37] M.J. Islam, Q.J. Wu, M. Ahmadi, M. Sid-Ahmed, et al., Investigating the performance of Naive–Bayes classifiers and k-nearest neighbor classifiers, in: Convergence Information Technology, 2007. International Conference on, IEEE, 2007, pp. 1541–1546.
[38] Y. Liao, V.R. Vemuri, Use of k-nearest neighbor classifier for intrusion detection, Computers & Security 21 (5) (2002) 439–448.
[39] N. Sakthivel, B.B. Nair, M. Elangovan, V. Sugumaran, S. Saravanmurugan, Comparison of dimensionality reduction techniques for the fault diagnosis of mono block centrifugal pump using vibration signals, Engineering Science and Technology, an International Journal 17 (1) (2014) 30–38.